α-decay properties of ^{200,202}Fr

L. Ghys,[1,2,*] A. N. Andreyev,[3,4] M. Huyse,[1] P. Van Duppen,[1] S. Antalic,[5] A. Barzakh,[6] L. Capponi,[7] T. E. Cocolios,[1,8,9]
J. Cubiss,[3] X. Derkx,[7,10] H. De Witte,[1] J. Elseviers,[1] F. P. Hessberger,[11,12] Z. Kalaninová,[5,13] U. Köster,[14] J. F. W. Lane,[7]
V. Liberati,[7] S. Mitsuoka,[4] Y. Nagame,[4] K. Nishio,[4] S. Ota,[4] D. Pauwels,[2] R. D. Page,[15] L. Popescu,[2] D. Radulov,[1]
M. M. Rajabali,[1] E. Rapisarda,[8] K. Sandhu,[7] V. L. Truesdale,[3] P. Van den Bergh,[1] and Y. Wakabayashi[4,16]

[1]*KU Leuven, Instituut voor Kern- en Stralingsfysica, B-3001 Leuven, Belgium*
[2]*Belgian Nuclear Research Center SCK•CEN, Boeretang 200, B-2400 Mol, Belgium*
[3]*Department of Physics, University of York, York YO10 5DD, United Kingdom*
[4]*Advanced Science Research Center, Japan Atomic Energy Agency, Tokai-Mura, Naka-gun, Ibaraki, 319-1195, Japan*
[5]*Department of Nuclear Physics and Biophysics, Comenius University, 84248 Bratislava, Slovakia*
[6]*Petersburg Nuclear Physics Institute, NRC Kurchatov Institute, RU-188300 Gatchina, Russia*
[7]*School of Engineering, University of the West of Scotland, Paisley PA1 2BE, United Kingdom*
[8]*PH Department, CERN, CH-1211 Genève 23, Switzerland*
[9]*School of Physics and Astronomy, The University of Manchester, M13 9PL, United Kingdom*
[10]*LPC, ENSICAEN, Université de Caen Basse Normandie, CNRS/IN2P3-ENSI, F-14050, France*
[11]*Gesellschaft für Schwerionenforschung, Planckstrasse 1, D-64291 Darmstadt, Germany*
[12]*Helmholtz Institut Mainz, D-55099 Mainz, Germany*
[13]*Laboratory of Nuclear Problems, JINR, 141980 Dubna, Russia*
[14]*Institut Laue Langevin, 71 avenue des Martyrs, F-38042 Grenoble Cedex 9, France*
[15]*Department of Physics, Oliver Lodge Laboratory, University of Liverpool, Liverpool L69 7ZE, United Kingdom*
[16]*RIKEN Nishina Center for Accelerator Based Science, Wako, Saitama 351 0198, Japan*

Background: The neutron-deficient lead region provides a range of nuclear phenomena, including isomerism at low energies. This phenomenon can be studied by α decay because the degree of hindrance of α decay provides information on the change in nuclear structure of connected states.

Purpose: The aim of this work was to investigate the α-decay properties of ^{200,202}Fr and daughter products.

Method: Neutron-deficient francium nuclei are produced at ISOLDE-CERN bombarding a UC$_x$ target with 1.4 GeV protons. Surface ionization and mass-separation techniques were employed to provide a pure radioactive ion beam at a radiation-detection setup.

Results: Due to the very high statistics and the high beam purity, improved decay data for ^{202}Fr and its daughters were obtained. In particular, this data set allowed us to identify many fine-structure α lines with a relative reduced α-decay width up to five orders of magnitude lower as the strongest ground-to-ground state or isomeric-to-isomeric state α-decay transition. In addition, several half-life values were extracted with similar or better precision as compared with the literature.

Conclusions: The observation of crossover transitions positioned the isomeric high-spin level of ^{198}At at an excitation energy of 265(3) keV. Half-life values of 4.47(5) s and 1.28(10) s were extracted for the ground state and isomeric state of ^{198}At and 52(3) ms for the ground-state decay of ^{200}Fr. Furthermore, α-decay schemes for ^{202}Fr and its daughter ^{198}At could be constructed.

I. INTRODUCTION

The neutron-deficient nuclei around the $Z = 82$ shell closure exhibit a variety of interesting nuclear structure and decay phenomena. Examples are shape coexistence, isomerism

---

*lars.ghys@sckcen.be

at low excitation energies [1,2], and the two-step decay process of β-delayed fission (βDF) [3]. Measuring the radioactive decay of these isotopes provides insights into these phenomena and can be used to unravel their decay schemes, which can be rather complex in the case of odd-odd nuclei. For example, the observation of fine-structure α-decay transitions and studying the degree of their hindrance allows low-energy states to be identified and their configuration to be studied (see, e.g., Refs. [4–6]). This paper reports on a detailed α-decay study of ^{200,202}Fr at the mass separator ISOLDE. The βDF properties of these isotopes, derived from the same data set, have been published elsewhere [7].

The α decay of ^{200}Fr was first observed after fusion-evaporation reactions at the recoil separator GARIS at RIKEN. An α-decay transition at $E_\alpha = 7500(30)$ keV with a half-life of 570^{+270}_{-140} ms was deduced from the six correlated events [8]. A similar experiment, with also six events associated with the α decay of ^{200}Fr, was performed at the RITU separator at the university of Jyväskylä [9]. An α line at $E_\alpha = 7468(9)$ keV, with a very different half-life of 19^{+13}_{-6} ms, was reported. A later experiment at ISOLDE (CERN), with higher statistics, reported $E_\alpha = 7473(12)$ keV and $T_{1/2} = 49(4)$ ms [10]. The latter values are in agreement with the results from a recent experiment at the velocity separator SHIP in GSI-Darmstadt, from which $E_\alpha = 7470(5)$ keV and $T_{1/2} = 46(4)$ ms were deduced [11]. Based on the unhindered decay to the (3^+) ground state of ^{196}At and the systematics in neighboring odd-odd nuclei, a spin and parity of (3^+) is tentatively assigned to the ground state of ^{200}Fr.

In the case of ^{202}Fr, one α-decay branch at 7251(10) keV was first observed at ISOLDE-CERN [12] with a half-life of 0.34(4) s. However, a doublet structure of this line, corresponding to two α-decaying isomeric states in ^{202}Fr, was later suggested by Huyse *et al.* in a study at the Leuven Isotope Separator LISOL [5]. Tentative spin assignments of (3^+) and (10^-) were suggested for the ground and isomeric state respectively, by analogy with its daughter products ^{198}At and ^{194}Bi. This inference was later confirmed by using α-α correlation techniques at recoil separators [9,11,13,14]. In a more recent study at SHIP [11], α-decay energies of 7238(5) keV and 7226(5) keV and corresponding half-lives of 372(12) ms and 286(13) ms were measured for the low-spin and high-spin isomeric states, respectively. A mass-spectrometry experiment at ISOLTRAP (ISOLDE, CERN) confirmed the order of these isomeric levels in ^{202}Fr and placed the high-spin isomer at an excitation energy of 281(17) keV with respect to the low-spin ground state [15]. Recently, the hyperfine structure of ^{202}Fr was studied by using the Collinear Resonance Ionization Spectroscopy (CRIS) experiment at ISOLDE. In particular, magnetic-moment measurements further support the spin assignment of (3^+) and (10^-) for the ground and isomeric state, respectively [16].

In this work, previously unknown α-decay fine structure is reported in the decay chain of ^{202}Fr-^{198}At-^{194}Bi, allowing new low-lying excited levels to be identified in both ^{198}At and ^{194}Bi. Furthermore, crossover transitions between the isomeric level in ^{202}Fr and the ground state in ^{198}At were observed, providing an independent and more precise measurement of the excitation energy of the isomeric state in ^{202}Fr. New half-life values, with similar or better precision as compared with previous studies, were measured for ^{198g,m}At and ^{200}Fr.

II. EXPERIMENTAL SETUP

This work analyzes experimental data acquired at the ISOLDE isotope separator at CERN. A detailed description of the experimental setup is provided in Refs. [7,17] and references therein. The ^{200,202}Fr isotopes are formed in spallation reactions of a pulsed proton beam with an energy of 1.4 GeV on a 50 g/cm^2 thick UC$_x$ target. The proton pulses (3×10^{13}
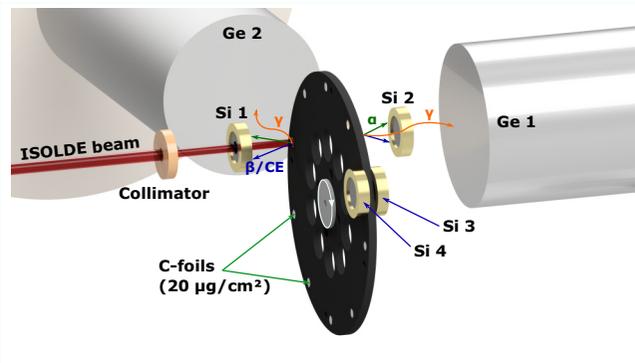

FIG. 1. A schematic view of the windmill detection setup. A radioactive beam from ISOLDE was implanted in one of ten carbon foils of $\sim$20 μg/cm^2 thickness, mounted on a rotatable wheel. Four silicon detectors were employed for the detection of electrons, α and fission particles. Two germanium detectors were placed outside the vacuum chamber for γ-ray detection. Illustration from Ref. [18].

protons per pulse) on target were separated by one or multiple periods of 1.2 s and are arranged in a repeated sequence with a duration between 14.4 and 50.4 s, called a supercycle (SC). After diffusion and effusion from the target, francium atoms were ionized through surface ionization in the hot cavity. The ions were then accelerated to a kinetic energy of 30 keV and subsequently mass separated by the high-resolution separator (HRS). The purified ion beam was transported into a "windmill" detection setup, where it was implanted on one of ten 20-μg/cm^2-thick carbon foils, mounted on a rotatable wheel. A schematic view of this setup is given in Fig. 1. At mass $A = 200$, due to the short half-life of ^{200}Fr, implantation was only allowed for 200 ms after the arrival of a proton pulse in order to reduce contamination of longer-living products. In the case of mass $A = 202$, implantation was stopped 1 s after
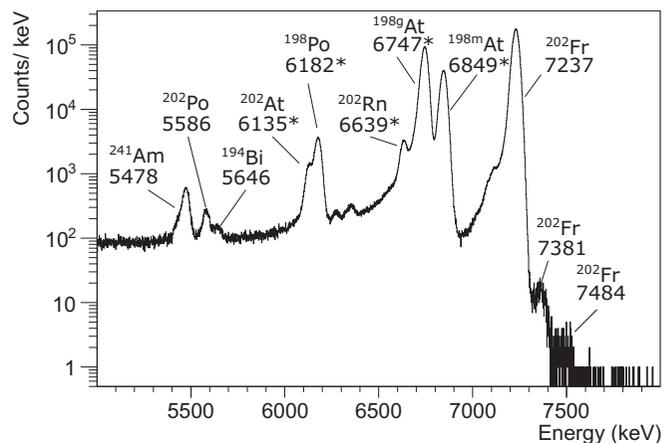

FIG. 2. Relevant part of the α-sum spectrum as recorded by the silicon detectors Si1 and Si2 at mass $A = 202$. Energies are given in keV and the lines used for energy calibration are marked with an asterisk (*) and taken from the literature [11,20,21]. The α line at 5478 keV is from ^{241}Am calibration sources, mounted on the wheel of the windmill.
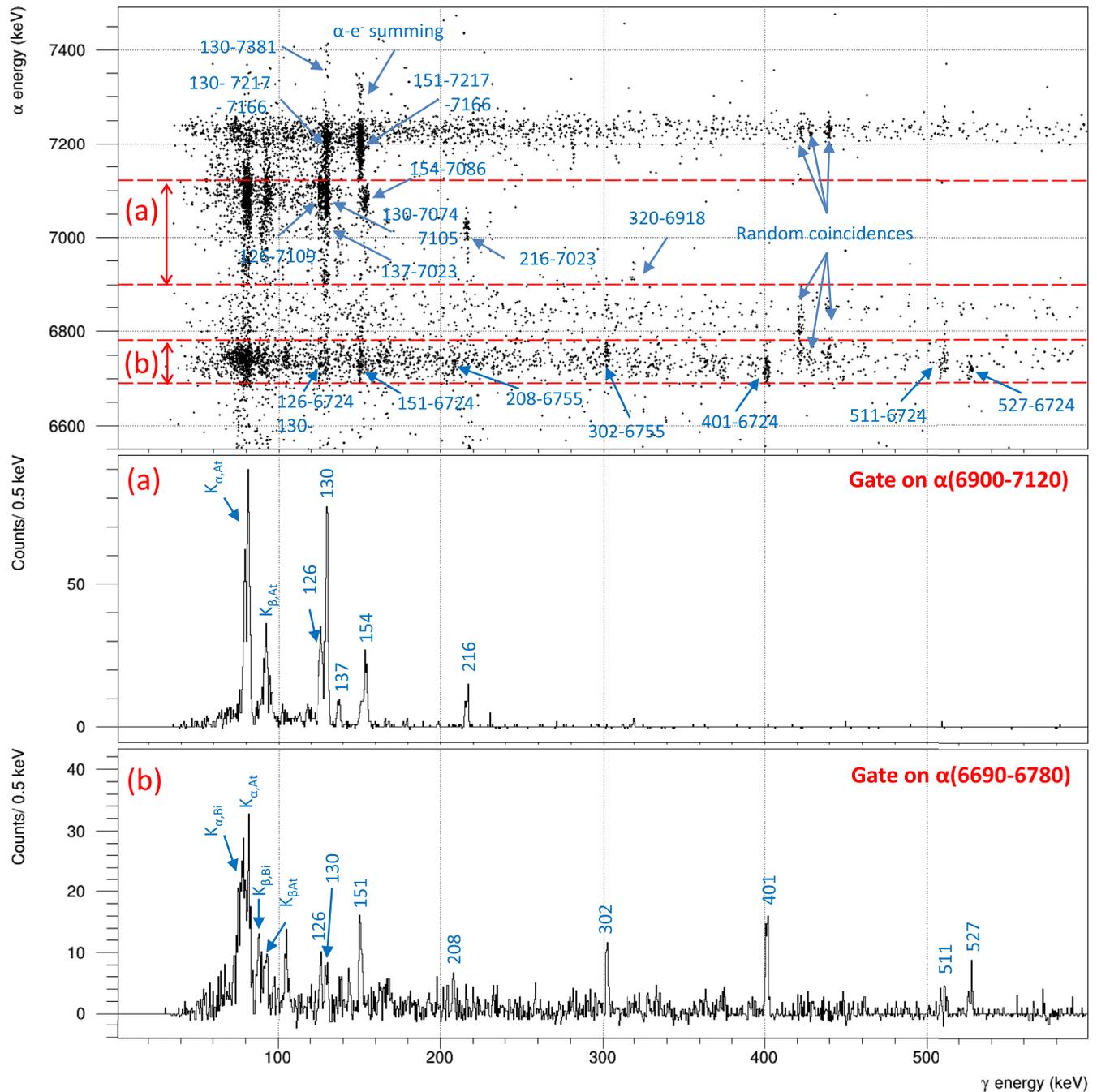
FIG. 3. The top panel depicts part of the prompt α-γ coincidences, relevant for the decay of ^{202}Fr, observed between the detectors Si1 and Si2 at the implantation position and the germanium detector Ge1. The width of the time gate was set to 600 ns. The identified α-γ groups are denoted with their respective energies in keV. Panels (a) and (b) show the random-subtracted γ-energy spectra coincident with the ranges of α-decay energies indicated by the broken red dotted lines on the upper plot. The energies of the γ lines are given in keV.

a proton pulse hit the target, sufficient to measure the decay of ^{202}Fr for approximately three half-lives. Two Si surface-barrier detectors (denoted by Si1 and Si2) with a depletion thickness of 300 μm were placed in close geometry at the implantation position. The detector upstream of the beam (Si1) was annular with an active area of 450 mm^2, excluding the hole with diameter of 8 mm, while the other detector (Si2) was circular with an active area of 300 mm^2. In total, these

detectors covered a solid angle of about 51% [17]. At the end of one SC, the irradiated foil could be turned towards the decay position, between a pair of PIPS Si detectors (Si3 and Si4) with an active area of 300 mm^2 and depletion thickness of 300 μm. Meanwhile, implantation continued on a fresh foil. The full width at half maximum (FWHM) for single α lines in the range of 5 to 8 MeV is approximately 33 keV. The silicon detectors were calibrated by using known

energies of α-decay lines in the energy spectra. The α decay of an implanted nucleus will cause a significant recoil of the daughter nucleus, altering its position in the carbon foil or even ejecting it from the foil with possible implantation on Si1 [19]. This so-called recoil-effect was taken into account in this work by introducing a (conservatively estimated) systematic calibration error of 8 keV on alpha-decay energies.

Two single-crystal high-purity germanium (HPGe) detectors (denoted Ge1 and Ge2), with a typical energy resolution (FWHM) of 2.5 keV at a γ energy of 1.3 MeV, were placed outside the vacuum chamber. Efficiency and energy calibrations were performed with standard sources of ^{60}Co, ^{133}Ba, ^{137}Cs, ^{152}Eu, and ^{241}Am (see also Ref. [17]). The detector Ge1, placed at $0°$ with respect to the beam direction and at about 1 cm behind the foil, had an absolute photopeak detection efficiency of 4.9(3)% for the 662 keV γ line of ^{137}Cs. Detector Ge2, positioned at a $90°$ angle and at roughly 3 cm from the foil, had a photopeak efficiency of 0.81(5)% at 662 keV [17].

Both the energy and timing information of the detector signals were stored on an event-by-event basis using digital gamma finder (DGF) modules. Events are periodically read out from a local buffer to a PC, during which acquisition is stopped. For this reason, dead-time effects should be considered when determining half-lives (see also Ref. [17]).

III. RESULTS

A. ^{202}Fr $\rightarrow$ ^{198}At

Figure 2 shows the summed energy spectrum of α decays, as recorded by Si1 and Si2 at mass $A = 202$. Only α particles originating from ^{202}Fr or its decay products ^{202}Rn, ^{198,202}At, ^{198,202}Po, and ^{194}Bi were identified.

The α peak at 7237(8) keV is associated with the known doublet of dominant α-decay lines from ^{202}Fr, depopulating its ground and isomeric state. This value is consistent with the corresponding energies observed in the recent SHIP experiment for the ground and isomeric state at 7238(5) and 7226(5) keV, respectively. Since our current setup does not allow separation of the isomeric or ground-state decays, the α-energy values from SHIP are adopted in the remainder of this article.

Although the α spectrum shows solely α lines from ^{202}Fr and its daughter products (see Fig. 2), the singles γ-ray spectrum is largely dominated by γ rays from contaminating ^{202}Tl nuclei, ionized through surface ionization (see also Ref. [17]). For this reason, only γ spectra in prompt coincidence with α-decay transitions could be used in the analysis.

Figure 3 gives part of the α-γ coincidences observed at mass $A = 202$, showing also relevant (random-subtracted) projections on the γ-ray-energy axis. This figure only depicts the part relevant for the α decay of ^{202}Fr. Table I gives a list of all identified α-γ coincidence pairs in the decay of ^{202}Fr, including their (relative) intensities.

Figure 3 shows two intense γ lines at 130.0(1) and 150.8(1) keV coincident with α particles in the α-energy region 7150–7250 keV. From the projected α spectrum, two separate α lines at 7166(8) and 7217(8) keV were found in

TABLE I. Summary of α-γ coincident pairs observed in Fig. 3 and attributed to the α decay of ^{202}Fr. The relative intensities $I_{\alpha\gamma,\mathrm{rel}}$, corrected for the detection efficiency, are given with respect to the most intense α-γ coincident pair at $\alpha(7217)$-$\gamma(151)$. When possible, the spin and parity J^{π} of the initial state, relative α-decay intensity I_{α}, and reduced α-decay width δ_{α}^2 are given for the respective α lines. I_{α} is given with respect to the most intense α decay lines at 7238 and 7226 keV.

E_{α} (keV)	J^{π}	I_{α} (%)	δ_{α}^2 (keV)	E_{γ} (keV)	$I_{\alpha\gamma,\mathrm{rel}}$
6724(8)	(10^-)	0.10(3)	3.2(9)	126.3(1)	5(1)
				130.0(1)	5(2)
				150.8(1)	9(2)
				401.4(1)	26(3)
				511(3)	8(2)
				527.3(2)	11(2)
6755(8)				207.8(2)	4(1)
				302.1(1)	12(2)
6918(10)				319.7(7)	4(1)
7012(9)				137.0(4)	5(1)
7023(8)				215.9(2)	10(2)
7074(9)				130.0(1)	32(7)
7086(8)	(3^+)	0.03–0.11	0.03–0.12	154.2(3)	30(3)
7105(8)	(3^+)	0.09(2)	0.08(2)	130.0(1)	29(6)
7109(8)	(10^-)	0.28–0.53	0.35–0.64	126.3(1)	37(4)
7166(8)	(10^-)	0.06(1)	0.05(1)	130.0(1)	14(3)
				150.8(1)	26(4)
7217(8)	(10^-)	0.23(5)	0.12(3)	130.0(1)	39(4)
				150.8(1)	100
7226(5)[a]	(10^-)	100	48(3)		
7238(5)[a]	(3^+)	100	33(2)		
7381(26)	(10^-)	0.014(6)	0.0020(10)	130.0(1)	2.0(8)
7484(32)	(10^-)	<0.008	$<5 \times 10^{-4}$		

[a]Values from Ref. [11].

coincidence with these γ lines. These findings are consistent with the results from an in-beam study of ^{198}At at RITU, where γ lines with energies of 130.0(1) keV and 151.7(2) keV were correlated with the ground-state α decay of ^{198}At [22]. The analysis of α-γ-γ coincidences (see Fig. 4) shows that
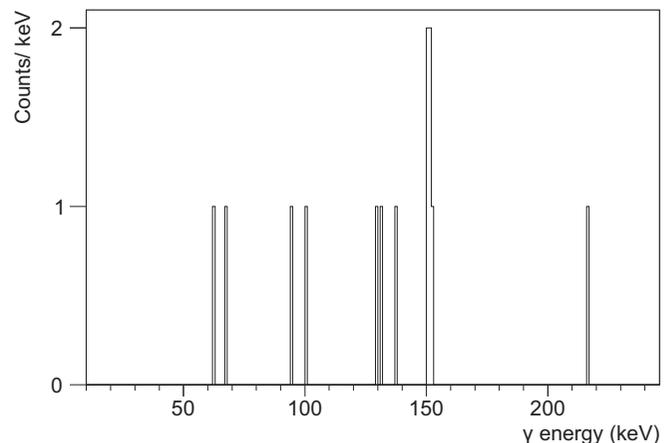
FIG. 4. γ-energy spectrum in prompt coincidence with pairs of coincident $\alpha(7217)$-$\gamma(130)$.

^{202}Fr

^{198}At

^{194}Bi

286(13) ms (10$^-$)
253(8)
0   372(12) ms   (3$^+$)

E_α [keV] 7238(5)* 7086(8) 7105(8) 7484(32) 7381(26) 7217(8) 7166(8) 6724(8) 7109(8) 7226(5)*
I_α [%]   100   0.03-0.11 0.09(2) < 0.008   0.014(6) 0.23(5) 0.06(1) 0.10(3) 0.28-0.53 100
δ^2_α [keV] 33(2) 0.03-0.12 0.08(2) < 5 x 10^{-4} 0.002(1) 0.12(3) 0.05(1) 3.2(9) 0.35-0.64 48(3)

792(3)   (8$^-$)
(E2) 511(3)   (M1/E2) 401
(E2) 527
391(3)   (8$^-$,9$^-$)
334(7)   M1/E2 126
281   53(7)   (6$^-$)   265(3)   1.28(10) s   (10$^-$)
E1 151
154   130   (5$^+$)
154   E2(M1) 130   (3$^+$)

E_α [keV] 6322(12) 6338(8) 6753(8) 6849(5)*
I_α [%]   0.005(3) 0.09-0.13 0.05-0.34 100
δ^2_α [keV] 0.2(1) 3.3-4.8 0.04-0.28 36(4)

699(8)   686(8)
538   525
266(8)
161(8)   105   (10$^-$)

E_α [keV] 6275(8) 6361(9) 6535(8) 6358(8) 6747(5)*
I_α [%]   0.08(1) 0.008(2) 0.020(3) 0.11(1) 100
δ^2_α [keV] 1.6(3) 0.06(2) 0.034(5) 1.0(1) 26(1)

486   E2(M1) 103
M1(E2) 486   267   382
218   400   M1(E2) 181   400
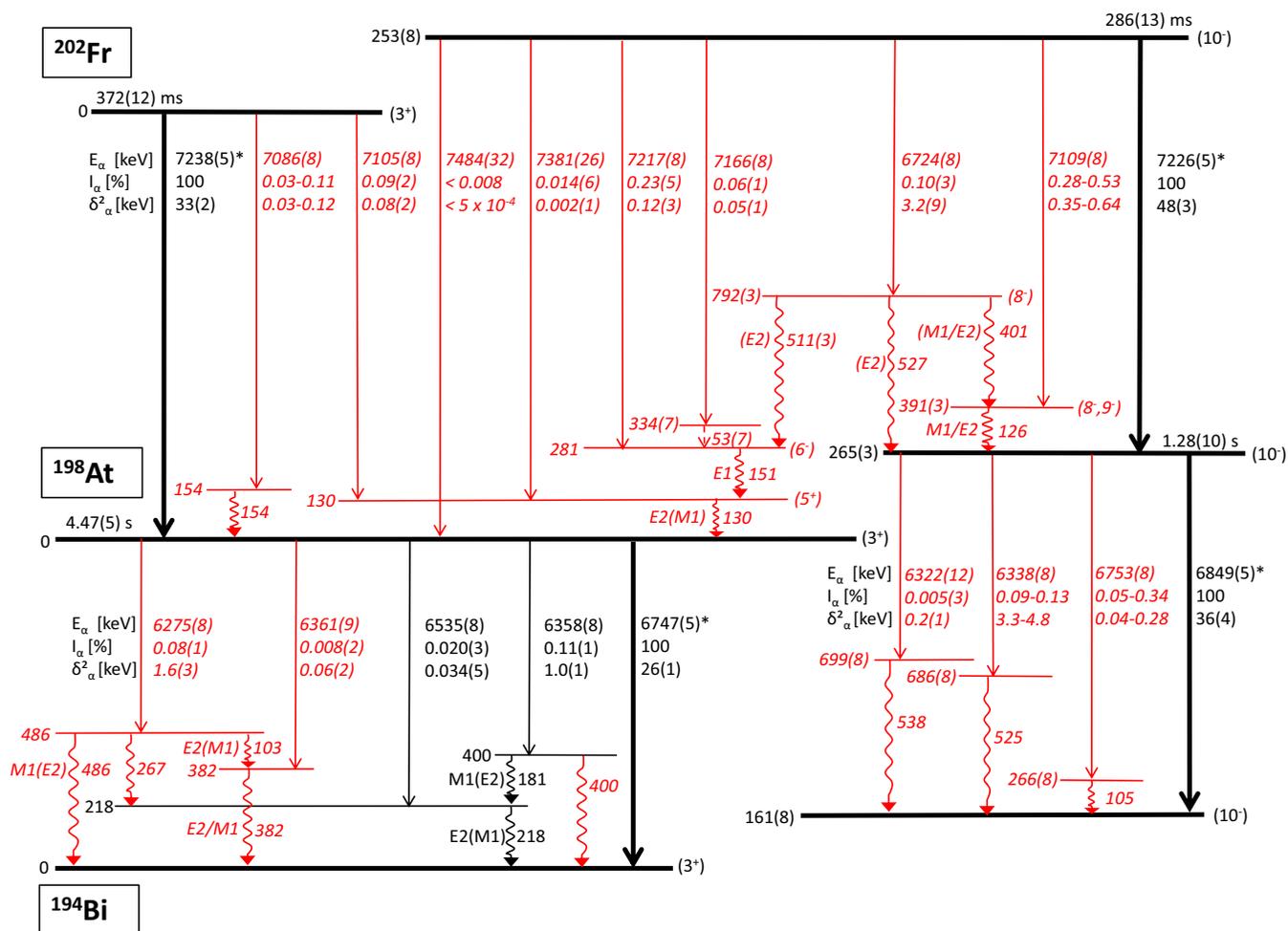E2/M1 382   E2(M1) 218
0   (3$^+$)

FIG. 5. The α-decay scheme of ^{202}Fr and its daughter ^{198}At as deduced from this work. All energies are given in keV. The yet-unobserved transition of 53(7) keV following the α decay of ^{202}Fr is indicated by a dashed arrow. The lifetimes of ^{202g,m}Fr are taken from Ref. [11]. The main α lines in the ^{198}At decay, marked with an asterisk (*), have been used for the energy calibration of the silicon detectors. Therefore, their energies are taken from the literature [11]. New transitions and levels are indicated in red, with the corresponding information written in italics.

the 151 keV γ line is in coincidence with both the 7217 keV α and the 130 keV γ transition. This observation confirms that the 130 and 151 keV γ lines are part of a cascade. Some coincidences of the 130 keV line with an α line at 7381(26) keV were also identified, suggesting that the 130 keV γ should be placed below the 151 keV transition in the level scheme. Note that, based on energy considerations, these α transitions must be crossover transitions from the isomeric state in ^{202}Fr that decay via γ emission to the ground state of ^{198}At. It is therefore assumed that the 151-130 keV γ cascade feeds the ground state directly from an excited level at 280.8(1) keV, populated by the 7217 keV α transition (see also Fig. 5). The 7166 keV line would then decay to a level at 334(7) keV, which deexcites by an unobserved transition of 53(7) keV to the level at 281 keV. The observed coincidences between α particles around 7310 and 151 keV γ rays in the top part of Fig. 3 are attributed to summing of conversion electrons from the 130 keV transition with the 7217 keV α particles, which suggests a significant conversion coefficient for the 130 keV transition. Following this scheme, the fine-structure α peak at around 7484(32) keV, observed in the

singles α spectrum of Fig. 2, might be (partially) attributed to the direct feeding of ^{198g}At from ^{202m}Fr. However, the α spectrum in the detectors Si3 and Si4 reveal a handful of events at higher energy ($E_\alpha > 7400$ keV) which can be attributed to contamination from isotopes of other masses. For this reason, only an upper limit could be given in Table I for the α intensity at 7484 keV.

Another α line at 6724(8) keV was found in coincidence with the γ rays at 130 and 151 keV [see Fig. 3(b)]. The same α line also shows coincidences with γ lines at 126.3(1), 401.4(1) and 527.3(2) keV, the last energy being the sum of the first two. It is likely that the 126 and 401 keV transitions form a cascade. In addition, the 126 keV γ line is coincident with another alpha at 7109(8) keV, placing this transition at the bottom of the cascade. Finally, another γ line at 511(3) keV, coincident with the 6724 keV α decay, could feed the energy level at 281 keV, which is deexcited by the 151-130 keV cascade to the ground state. The proposed decay scheme assumes that the level at 792(3) keV feeds both ground and isomeric states. From the decay scheme in Fig. 5 it is clear that the 792(3) keV can be placed 527 keV above the isomeric

state, fixing the excitation energy of the isomer in ^{198}At at 265(3) keV. Using this value as a starting point, the positions of the isomeric level in ^{202}Fr and ^{194}Bi could be determined as 253(8) and 161(8) keV, respectively, by using the energy of the direct α transitions (see also Fig. 10). A comparison with previous mass measurements follows in Sec. IV.

Figure 3 shows more γ lines in coincidence with the fine-structure α decay of ^{202}Fr, which are listed in Table I. Since isomeric separation is not feasible with the current setup, it is difficult to disentangle whether the γ lines should be attributed to the ground or isomeric-state. However, a γ line at 154 keV is probably feeding the ground state of ^{202}Fr directly, as is supported by energy considerations: $Q_{\alpha,\text{tot}} = Q_\alpha + E_\gamma$. This placement is justified by the observation of a 155.5(9) keV γ line in the in-beam study by Taylor and coworkers [22], which was correlated with the ground-state α decay of ^{198}At. As shown in Fig. 3 and Table I, a γ line at 130.0(1) keV is observed in coincidence with α-decay lines at 7074(9) and 7105(8) keV. The latter α line can be placed naturally in the decay scheme (Fig. 5), as the direct feeding from the ground state of ^{202}Fr to the level at 130 keV. After careful analysis of the α spectra by gating on the high- and low-energy part of the 130 keV line, it was found that this γ line is most probably a doublet. The α peak at 7074 keV should thus be coincident with another γ line at 130 keV, but slightly shifted in energy as compared with the 130.0(1) keV line. The α(7074 keV)-γ(130 keV) pair, along with several other α-γ pairs indicated in Table I, could not be placed in the current level scheme.

Because of the their prompt nature, all γ transitions observed in Fig. 3 are supposed to have multipolarities $E1$, $M1$, or $E2$ (or $M2$ for transitions with $E \gtrsim 400$). The multipolarities for several γ rays in cascade could be further determined by studying intensity balances. From the number of α-γ-γ coincidences $I_{\gamma1\gamma2} = 5$ (see Fig. 4), the total conversion coefficients α_{expt} could be approximated for the 130-151 keV cascade by using

$$\alpha_{1,\text{expt,tot}} = \frac{I_{\gamma2}(\text{Ge1})\epsilon_{\gamma1}(\text{Ge2}) + I_{\gamma2}(\text{Ge2})\epsilon_{\gamma1}(\text{Ge1})}{I_{\gamma1\gamma2}} - 1. \tag{1}$$

The γ rays in the cascade are denoted here by γ_1 and γ_2 and $\alpha_{1,\text{expt,tot}}$ is the total conversion coefficient of γ_1. $I_{\gamma2}(\text{Ge1,2})$ is the intensity corresponding to γ_2 observed in either Ge1 or Ge2 in the α-γ coincidence spectrum (Fig. 3, top panel). The photodetection efficiency of γ_1 in Ge1 and Ge2 is denoted by $\epsilon_{\gamma1}(\text{Ge1})$ and $\epsilon_{\gamma1}(\text{Ge2})$, respectively. An analogous equation can be used to determine $\alpha_{2,\text{expt,tot}}$. Equation (1) only gives an approximation since the summing of α particles and electrons in the same silicon detector or the summing of γ_1 and γ_2 in the same Ge detector are not considered. However, the bias induced by this effect is in this case small as compared with the statistical error induced by $I_{\gamma1\gamma2}$. Using Eq. (1), the total conversion coefficients of 1.5(11) and 0.1^{+5}_{-1} were determined for the 130 keV and 151 keV transitions, respectively. A comparison with calculated conversion coefficients α_{theo}, given in Table II, shows that the 151 keV transition most probably has an $E1$ multipolarity. A similar reasoning suggests a multipolarity of predominantly $E2$ for the 130 keV transition.

TABLE II. Experimental and theoretical conversion coefficients for the 130 and 151 keV γ transitions, observed after the α decay of ^{202}Fr to ^{198}At. The experimental total conversion coefficients $\alpha_{\text{expt,tot}}$ were determined from the number of α-γ-γ coincidences between both γ lines and the 7217 keV α line. Calculated total conversion coefficients $\alpha_{\text{theo,tot}}$ are taken from Ref. [23] for different multipolarities. In addition, the K conversion coefficient $\alpha_{\text{theo,K}}$ is also listed. "MP" stands for "multipolarity."

E_γ	$\alpha_{\text{expt,tot}}$	MP	$\alpha_{\text{theo,tot}}$	$\alpha_{\text{theo,K}}$
130.0(1)	1.5(11)	$E2$	2.57	0.36
		$M1$	5.73	4.64
150.8(1)	0.1^{+5}_{-1}	$E1$	0.17	0.13

The possible mixing ratio with multipolarity of $M1$, which mainly proceeds via K conversion, is considered limited due to the small amount of x rays observed in coincidence with the 7217 keV α line and the smaller experimental value for $\alpha_{\text{expt,tot}}$ in comparison with the calculated value α_{theo} for $M1$ transitions (see Table II).

The assignments of multipolarity for the 126-401 keV cascade can be determined by studying the intensity ratio of both γ lines. This method can also be employed to verify the multipolarities for the 130-151 keV cascade. For a cascade consisting of two γ transitions, denoted by γ_1 and γ_2, one has

$$\frac{1 + \alpha_2}{1 + \alpha_1} = \frac{I_{\gamma1}\epsilon_{\gamma2}}{I_{\gamma2}\epsilon_{\gamma1}}, \tag{2}$$

where α_1 and α_2 are the calculated total conversion coefficients [23] for γ_1 and γ_2, respectively for a specific multipolarity. The experimental γ intensities, in coincidence with the α line under consideration, are given by $I_{\gamma1}$ and $I_{\gamma2}$. Table III compares calculated versus experimental intensity ratios. In the case of the 151-130 keV cascade, the $E1$-$E2$ assignment is confirmed. For the 401 keV γ, a conversion coefficient of $\simeq 0$ can be assumed due to its relatively high energy. Based on this analysis, a mixed $M1/E2$ multipolarity is assumed for the 126 keV transition.

In Fig. 5, the proposed level scheme with the assigned α and γ transitions is depicted. The intensities of the fine-structure decays, I_α, are given relative to the most intense α-decay lines at 7238 and 7226 keV being respectively the

TABLE III. Calculated and experimental intensity ratios, as determined by Eq. (2), for identified γ cascades following the α decay of ^{202}Fr at 7217 and 6724 keV. Theoretical ratios are given for specific multipolarities (MP). In the case of the 401 keV transition, a small conversion coefficient was assumed. The most probable multipolarities are indicated in bold.

$E_{\gamma1}$-$E_{\gamma2}$ (keV)	$I_{\gamma1}/I_{\gamma2}$	MP $\gamma1$	MP $\gamma2$	$\frac{1+\alpha_2}{1+\alpha_1}$
150.8(1)-130.0(1)	2.5(3)	**$E1$**	**$E2$**	3.1
		$E1$	$M1$	5.8
401.4(1)-126.3(1)	4.9(12)	($\alpha_1 \simeq 0$)	$E1$	1.3
			$E2$	3.9
			$M1$	7.3

ground-to-ground state and isomer-to-isomer transitions. For most of the α fine-structure decay lines, the intensity of the α peak is calculated from the intensity of the α-γ coincident pairs, thereby taking into account the absolute efficiency of the Ge1 detector and the calculated conversion coefficients corresponding to the possible multipolarities of the transitions. For the 7484 keVα line, an upper limit for I_α was estimated from the singles α spectrum, thereby acknowledging the fact that some of the events at high energy could be from contaminating isotopes. Finally, reduced α-decay widths δ_α^2 were extracted by using the Rasmussen formalism [24]. It was assumed that the β branching ratio of both the ground and isomeric state in ^{202}Fr is close to zero. However, from the ^{202}Rn counts in the singles-α spectrum, see Fig. 2, a (small) overall β branching ratio b_β of 2.4(2)% could be determined for ^{202}Fr [17]. Since ground and isomeric states could not be separated with the current setup, it was assumed that b_β is sufficiently small in both ground-state and isomeric-state decays and that it does not alter significantly the calculated δ_α^2 in Table I.

Based on the proposed spin and parity assignments of the isomeric and ground states in the literature [5], the extracted multipolarities and decay widths of the α lines, tentative spin and parity assignments could be made for several newly found excited levels. Because of the $E2$ nature of the 130 keV γ line, the energy level at 130 keV should have the same parity as the 3^+ ground state, with a maximum change in spin of two. Since the reduced width of the 7381 keV α line is at least an order of magnitude larger as compared with the 7484 keV decay, the highest possible spin of 5^+ is assumed. The hindered 7105 keV α decay from the ^{202}Fr ground state to the level at 130 keV is also consistent with a spin change. A similar reasoning led to the assignment of 6^- for the 281 keV excited level, being depopulated with the 151 keV transition of $E1$ nature. The 792 keV excited level decays via the 511 and 527 keV γ lines. Due to their prompt nature, a maximum spin change of two can be assumed for these transitions. Since, based on tentative spin assignments, the 511 and 527 are feeding directly a (6^-) and (10^-) state respectively, a spin of eight is assumed. In addition, a negative parity is adopted because of the relatively low hindrance factor of the 6724 keV α, suggesting a similar configuration and thus same parity as the (10^-) isomeric level. This assignment also implies an $E2$ nature for both the 511 and 527 keV transitions.

B. ^{198}At $\rightarrow$ ^{194}Bi

As the half-lives of ^{198g,m}At are in the region of 1–4 seconds, the determination of their half-lives is more convenient by using Si3/Si4 at the decay position of the windmill. There is no new implantation at this position, implying that a pure decay curve can be measured. Due to the movement time of 0.8 s of the windmill, the short-lived ^{202}Fr is not present anymore at the decay position. Figure 6 shows the time distribution of α particles from the ground or isomeric state of ^{198}At with respect to time at which the implantation foil reaches the decay position. In addition, this spectrum is corrected for dead-time effects by using a 10 Hz pulser (see also Ref. [17]). Half-lives of 4.47(10) s and 1.28(10) s
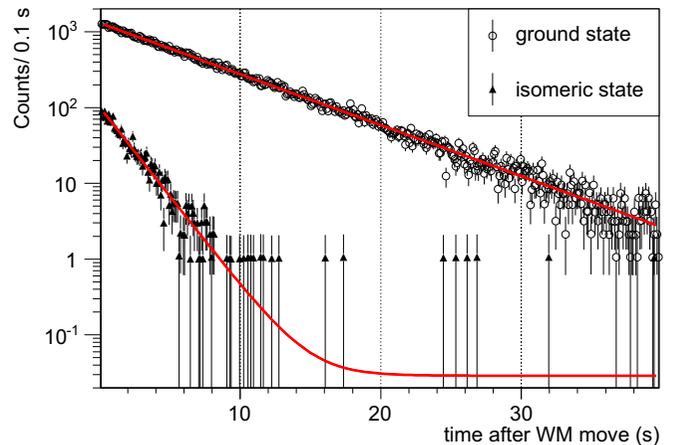

FIG. 6. Timing distributions of α particles, recorded by detectors Si3 and Si4, with respect to the movement of the windmill (WM). The data are corrected for dead-time effects, which were monitored by a 10 Hz pulser (see Ref. [17]). The closed triangles and open circles correspond to the α-decay lines of ^{198}At at 6753 keV (isomeric state) and 6854 keV (ground state). Fits to the data are shown by the red lines, yielding half-life values of 4.47(10) and 1.28(10) s for the ground and isomeric level, respectively.

were found for the ground and isomeric state, respectively. As shown in Table IV, the values from this work are in agreement with most previous measurements and have in general a better precision. It should be noted that the half-life of the ground state from Ref. [11] differs significantly from the values from this work and other measurements.

Figure 7 depicts the α-γ coincidence groups relevant for the α decay of ^{198}At. Table V gives an overview of the α-decay lines and prompt γ transitions which were attributed to the decay of ^{198}At. The α intensities I_α were again deduced from the intensities of the coincident γ rays. For the determination of the reduced α widths δ_α^2, α branching ratios of 97(3)% and 93(7)% for the ground and isomeric states in ^{198}At were considered, respectively [20].

Both the 218.2(1) keV and 181.4(1) keV γ lines reported in this work have been observed by Huyse *et al.* and are supposed to feed to the ground state of ^{194}Bi [5]; see also Fig. 5. These observations are confirmed by this work, where the 218 keV line is found in prompt coincidence with α lines at 6358(8) and 6535(8) keV and the 181 keV line is also coincident with the transition at 6358 keV. In addition, we

TABLE IV. Half-lives for the ground ($T_{1/2,g}$) and isomeric ($T_{1/2,m}$) state of ^{198}At from this measurement as well as values from the literature.

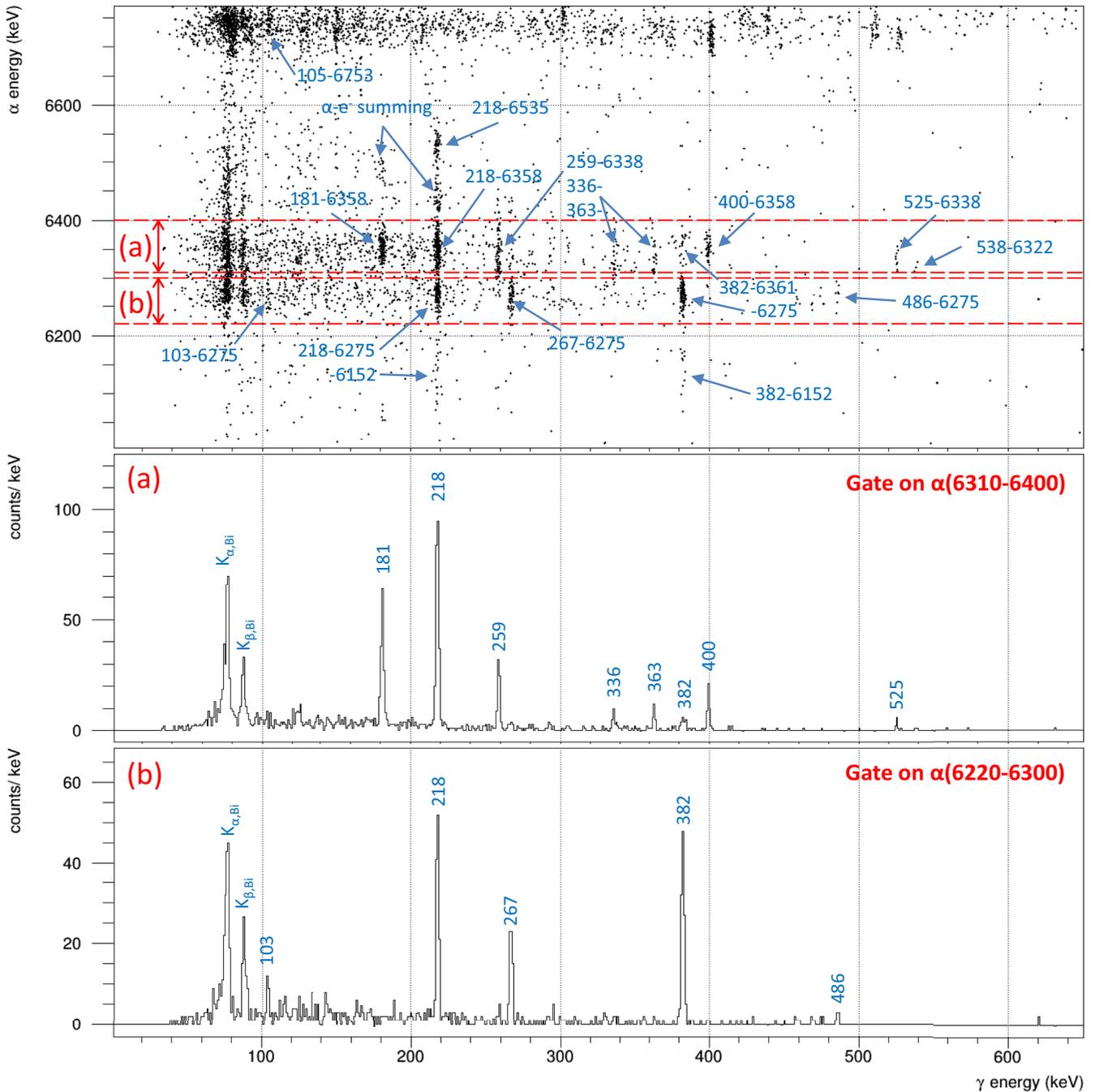| $T_{1/2,g}$ (s)	$T_{1/2,m}$ (s)	Reference
4.47(10)	1.28(10)	This work
3.0(1)	1.24(6)	[11]
3.8(4)	1.04(15)	[14]
$4.6^{+1.8}_{-1.0}$	$1.3^{+0.8}_{-0.3}$	[9]
4.2(3)	1.0(2)	[5]

FIG. 7. Similar to Fig. 3, but the range of the α-γ plot (top) and projections (a) and (b) are now relevant for the ^{198}At-^{194}Bi decay.

found that the latter α transition is coincident with a γ ray at 399.7(2) keV, corresponding to a direct γ decay to the ground state of ^{194}Bi. An apparent α peak at 6439 keV, coincident with the 218 keV γ has been identified as a summation peak of 6358 KeVα particles with the K-conversion electron in the decay of the 181 keV transition. In a similar way, the (weaker) α(6490 keV)-γ(181 keV) group is explained as summing with K-conversion electrons from the 218 keV transition.

Another, previously unobserved, α-decay line at 6275(8) keV is found in coincidence with γ transitions at 103.4(2), 218.2(1), 267.1(1), 382.4(1), and 485.8(7) keV.

Note that the sum of energies for the 103 and 382 keV lines on one hand and those at 218 and 267 keV on the other add up (within error bars) to the energy of the 486 keV γ line. These observations suggest two different γ-γ cascades and a single gamma depopulating in parallel an excited level at 486 keV. Since the level at 218 keV was already established, the 267 keV line is placed on top. A weak α line was found at 6361(9) keV in coincidence with the 382 keV line, placing the latter line at the bottom of the 103-382 keV cascade.

In addition, evidence was found for an α line at 6152(11) keV coincident with γ rays at 218(1) and

TABLE V. Similar to Table I, but for the α decay of ^{198}At. The relative intensities $I_{\alpha\gamma,\mathrm{rel}}$, corrected for the detection efficiency, are given with respect to the most intense α-γ coincident pair at $\alpha(6358)$-$\gamma(218)$.

E_α (keV)	J^π	I_α (%)	δ_α^2 (keV)	E_γ (keV)	$I_{\alpha\gamma,\mathrm{rel}}$
6152(11)	(3^+)			218(1)	6(2)
				382(1)	4(2)
6275(8)	(3^+)	0.08(1)	1.6(3)	103.4(2)	8(2)
				218.2(1)	39(5)
				267.1(1)	26(4)
				382.4(1)	61(7)
				485.8(7)	4(2)
6322(12)	(10^-)	0.005(3)	0.2(1)	538.3(4)	2.8(14)
6338(8)	(10^-)	0.09–0.13	3.3–4.8	258.8(1)	24(4)
				336.3(5)	15(3)
				363.6(2)	12(3)
				525.4(2)	5(2)
6358(8)	(3^+)	0.11(1)	1.0(1)	181.4(1)	52(6)
				218.2(1)	100
				399.7(2)	23(4)
6361(9)	(3^+)	0.008(2)	0.06(2)	382.4(1)	9(2)
6535(8)	(3^+)	0.020(3)	0.034(5)	218.2(1)	21(3)
6753(8)	(10^-)	0.05–0.34	0.04–0.28	104.5(2)	21(3)
6747(5)[a]	(3^+)	100	26(1)		
6849(5)[a]	(10^-)	100	36(4)		

[a]Energies from Ref. [11].

382(1) keV. We tentatively assign this fine-structure 6152 keV decay to a 600 keV level in ^{194}Bi, deexciting by a cascade of 218 and 382 keV transitions. It is not clear if one of these γ lines is the same as those feeding directly the 3^+ state. However, if our tentative assignment is correct, it follows that the 218 and/or 382 keV γ-ray peak must be a doublet. Due to the tentative nature of this decay path we decided not to add it to Fig. 5.

Some evidence of fine structure was also identified in the decay of the isomeric (10^-) state in ^{198}At. Three γ lines at 105, 525, and 538 keV were found in prompt coincidence with α-decay lines at 6753(8), 6338(8), and 6322(12), respectively. The energy balance suggests direct feeding of the (10^-) isomeric level in ^{194}Bi for all three cases. Finally, it seems that the same 6338 keV α line is also in coincidence with three other γ rays at 259, 336, and 363 keV, but their placement could not be determined. In any case, none of these transitions can be in cascade with each other since their sum is always higher than the 525 keV energy of the excited level. Although not shown in Fig. 5, these transitions were taken into account in the determination of the reduced α widths δ_α^2 in Table V.

As in the case of the ^{202}Fr-^{198}At decay, all γ transitions observed in Fig. 7 are supposed to have multipolarities $E1$, $M1$, or $E2$ (or $M2$ for transitions with $E \gtrsim 400$). For some cases, a more precise deduction was possible, such as for the 181 and 218 keV transitions in cascade. As mentioned earlier, the $\alpha(6439$ keV$)$-$\gamma(218$ keV$)$ group was identified as a strong α-e^- sum peak of K-conversion electrons from the 181 keV transition with 6358 keV α particles. The intensity is about 20% of the main $\alpha(6358$ keV$)$-$\gamma(218$ keV$)$ group, which

TABLE VI. Calculated and experimental intensity ratios for identified γ cascades following the α decay of ^{198}At, similar to Table III. In the case of the 382 keV transition, a small conversion coefficient was assumed.

$E_{\gamma1}$-$E_{\gamma2}$ (keV)	$I_{\gamma1}/I_{\gamma2}$	MP $\gamma1$	MP $\gamma2$	$\frac{1+\alpha_2}{1+\alpha_1}$
218.2(1)-181.4(1)	1.9(2)	**$E2$**	**$M1$**	2.2
		$M1$	$M1$	1.4
218.2(1)-267.1(1)	1.5(2)	$E2$	$E1$	0.8
		$E2$	$E2$	0.9
		$E2$	**$M1$**	1.2
382.4(1)-103.8(2)	8(2)	$(\alpha_1 \simeq 0)$	**$E2$**	7.0
		$M1$		10.4

would indicate a high (K-)conversion coefficient and thus a predominantly $M1$ nature for the 181 keV line. In a similar way, a group at $\alpha(6490$ keV$)$-$\gamma(181$ keV$)$ can be attributed to K-conversion electrons from the 218 keV transition summing with 6358 keV α particles. The intensity of this group is about 10 times smaller than the main $\alpha(6358$ keV$)$-$\gamma(181$ keV$)$ coincident pair, indicating a smaller but non-negligible conversion coefficient for this transition. This observation would already exclude the possibility of an $E1$ transition and thus point to an $E2$ transition, with some $M1$ admixture. Another hint for a modest conversion coefficient is the observation of K x rays in prompt coincidence with the 6535 keV α line, decaying to the 218 keV excited level in ^{194}Bi. The intensity ratio between K x rays and 218 keV γ rays, corrected for detection efficiency and background, yields an absolute K conversion coefficient $\alpha_{K,\mathrm{expt}}$ of 0.5(3). This value lies between the theoretical $\alpha_{K,\mathrm{theo}}$ of $E2$ and $M1$ at 0.14 and 0.91, respectively [23].

Table VI shows intensity balances, calculated using Eq. (2), for different cascades. The assignment of $M1$ for 181 keV and $E2(M1)$ for the 218 keV could be confirmed (see Table VI). In the case of the 218-267 keV cascade, a dominant $M1$ multipolarity was deduced for the latter transition. For the 103 keV line, in cascade with the 382 keV transition, a (predominant) $E2$ nature could be established. Due to the relatively high energy of the 382 keV line, all considered multipolarities yield small calculated conversion coefficients, prohibiting further assessment. Since there are no crossover transitions between the low- (3^+) and high-spin (10^-) isomer, no (tentative) spin assignments could be made, as was the case for ^{202}Fr.

C. ^{200}Fr $\rightarrow$ ^{196}At

The α spectrum, as recorded at the implantation position for $A = 200$, is shown in Fig. 8. The decay lines of ^{200}Fr and its α-daughter products ^{196}At and ^{192}Bi can be identified in this spectrum. Also, α-decay lines of contaminating nuclei of ^{200}At and daughter ^{200}Po are observed. Using the current data set, the energy of the main α line of ^{200}Fr is determined at 7466(12) keV, consistent with literature values; see Table VII. The uncertainty value is rather large, due to the systematic error introduced by the previously mentioned recoil effect, which could shift the energy of the α particles from the ^{196}At α-decay line. The main α-decay line at 6902 keV of the
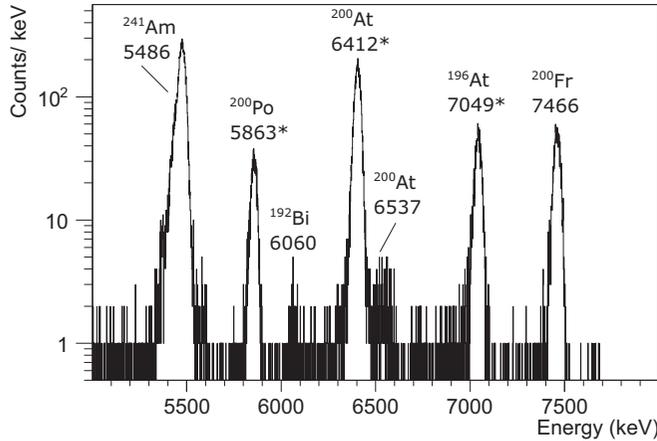
FIG. 8. Relevant part of the singles α spectrum as recorded by the silicon detectors Si1 and Si2 at the implantation station at mass 200. Energies are given in keV and the lines used for energy calibration, taken from the literature [25,26], are marked with an asterisk (*). The α line at 5.486 MeV is from ^{241}Am calibration sources, mounted in the wheel of the detection system.
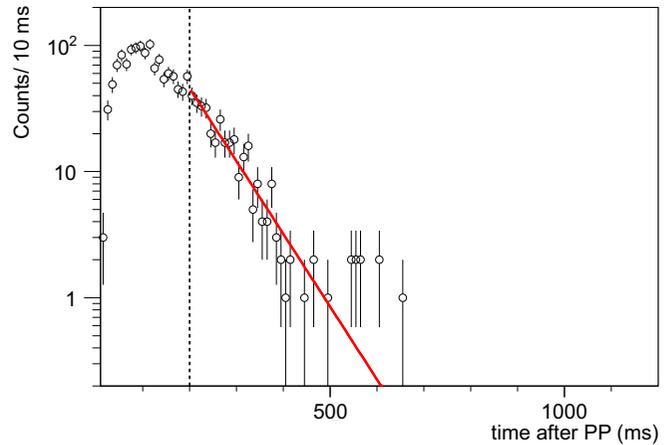

FIG. 9. Timing behavior of α particles with energies between 7350 and 7550 keV, attributed to the decay of ^{200}Fr, with respect to the arrival of a proton pulse (PP) on the ISOLDE target. Implantation is stopped after 200 ms, as indicated by the dotted line. The data are fit with a simple exponential curve without background, shown by the red line, yielding a half-life of 52(3) ms for ^{200}Fr.

β-decay daughter ^{200}Rn was not observed in the α spectrum of Fig. 8. Therefore, only an upper limit for the β branching ratio of ^{200}Fr is extracted at $b_\beta < 2.1\%$.

Figure 9 depicts the time behavior of the α rate from the 7466 keV decay line, detected by Si1 and Si2, with respect to the arrival of a proton pulse. After 200 ms of implantation, an exponential curve corresponding to the decay of ^{200}Fr is observed in Fig. 9. A log-likelihood based fitting method yields a half-life of 52(3) ms, slightly exceeding the most recent value from Ref. [11] (see Table VII).

IV. DISCUSSION

The newly observed crossover transitions in the ^{202}Fr-^{198}At α decay between ground and isomeric states provides an independent, and more precise, measurement of the excitation energy of the high-spin isomeric level in ^{198}At at 265(3) keV [cf. value of 282(12) deduced from previous study [15]; see below]. Because of the connecting α lines to both parent and daughter nuclei (see Fig. 10), excitation energies of isomeric levels could be deduced for the nuclei ^{206}Ac-^{202}Fr-^{198}At-^{194}Bi-^{190}Tl. In Table VIII, the values extracted from this work are compared with values obtained from dedicated mass measurements on ^{190m}Tl and

TABLE VII. Comparison of previous measurements and this work for the half-life values $T_{1/2}$, mean α energies and reduced widths δ_α^2 of the main decay line of ^{200}Fr.

Energy (keV)	$T_{1/2}$ (ms)	δ_α^2	Reference
7466(12)	52(3)	44(5)	This work
7470(5)	46(4)	48(5)	[11]
7473(12)	49(4)	44(5)	[10]
7468(9)	19^{+13}_{-6}	120^{+80}_{-40}	[9]
7500(30)	570^{+270}_{-140}	$3.1^{1.6}_{-1.0}$	[8]

^{198g}At and by using the linking α-decay energies [15]. For consistency, the excitation energies from Ref. [15] were recalculated by using the most recent α-decay energies from Fig. 10. This work confirmed the ordering of the low-spin and high-spin isomers in these nuclides as being, respectively, the ground and levels. More precise values for the excitation energies were obtained, which are slightly lower than those (recalculated) from Ref. [15]. These values serve as an important input to theoretical studies on, e.g., shape coexistence in this region or on β-delayed fission. For example, using the information from Table VIII and the evaluated masses of ^{202}Rn and ^{202}Fr [27], Q_β values for both the ground and isomeric states of ^{202}Fr can be fixed, with
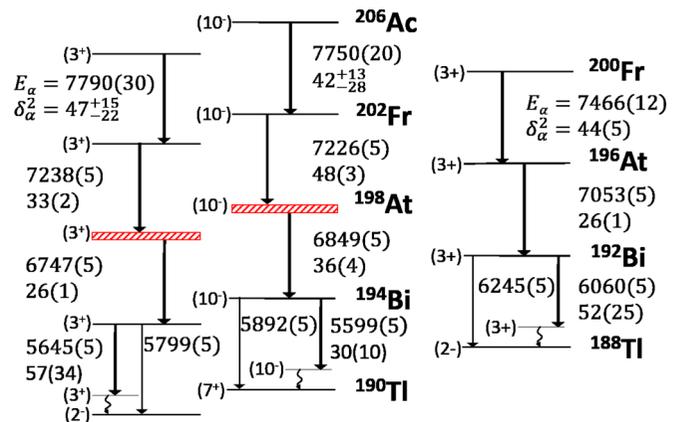

FIG. 10. Schematic view of the main α-decay chains of the ground and isomeric states of ^{206}Ac up to ^{190}Tl (left) and for ^{200}Fr-^{188}Tl (right). The α-decay energies and reduced widths are given in keV and taken from the literature [4,11,13,28] or from this work (for ^{200}Fr decay). The excitation energy of the isomer in ^{198}At (cf. red hatched lines) has been used as the reference to calculate the excitation energies of parent and daughter nuclei in Table VIII.

TABLE VIII. The excitation energies of the isomeric levels in the ^{206}Ac-^{190}Tl α-decay chain extracted from this work are compared with the values from Ref. [15], but recalculated using the α-decay energies from Fig. 10.

Nuclide	Excitation energy (keV)	
	Literature [15]	This work
^{190}Tl	83(11)	66(10)
^{194}Bi	178(12)	161(8)
^{198}At	282(12)	265(3)
^{202}Fr	270(14)	253(8)
^{206}Ac	229(39)	214(37)

good precision, at 9.37(2) and 9.62(2) MeV, respectively. These values can be used to model, e.g., the β-delayed fission (βDF) process of ^{202}Fr and possible differences in the properties of βDF from its ground and isomeric state. A first study of βDF fission properties of ^{202}Fr has already been performed [7], but βDF properties for ground and isomeric state could not be disentangled. However, such separation could be feasible in future experiments using, e.g., resonance ionization spectroscopy techniques [16].

Due to the high statistics obtained in this work, several new fine-structure α-decay lines, some of them in coincidence with γ decays, were found in the decay chain of ^{202}Fr-^{198}At-^{194}Bi. The reduced widths δ_α^2 extracted here were compared with those from other odd-odd Bi, At, and Fr nuclei in the region $N < 126$. In Fig. 11, the δ_α^2 values (on a logarithmic scale) for this region are summarized by plotting them against the mass number A. Some interesting systematic trends can be uncovered. First, the vast majority of isotopes studied have only one unhindered decay per isomer, with $10 \lesssim \delta_\alpha^2 \lesssim 100$. Some exceptions are found in the decay of ^{186}Bi [29] and

^{192}At [30], where multiple α-decay lines for one of the isomers appear to be unhindered ($\delta_\alpha^2 \gtrsim 10$). In addition, Fig. 10 shows the δ_α^2 values of the unhindered decays in the α-decay chains of ^{206}Ac and ^{200}Fr up to ^{190}Tl and ^{188}Tl, respectively. Within error bars, a decrease of δ_α^2 can be seen when moving down in Z towards the $Z = 82$ shell closure, both for the (10^-) and (3^+) states. This trend is somehow expected, as a similar trend was also observed for the even-even cases in this region ($Z > 82$ and $N < 126$) [31]. Second, the distribution of the δ_α^2 values for these odd-odd nuclei (see Fig. 11) shows a distinct dip between the unhindered ($\delta_\alpha^2 \gtrsim 10$) and hindered α decays. On average, the latter are hindered by more than factor of 100 as compared with the unhindered decays. It thus appears that the unhindered α decay in the region of $Z > 82$ and $Z < 126$ happens almost exclusively between members of the same proton-neutron configuration in parent and daughter, while any spin change, even within the same multiplet, leads to a very strong hindrance. As a consequence, most multiplet states in this region can be considered relatively pure. A similar observation was already made in a previous study [4] and can now be confirmed with a much larger volume of data, with the exceptions noted above.

V. CONCLUSIONS

In this paper, the α-decay properties of the odd-odd neutron-deficient isotopes ^{200,202}Fr were studied in detail thanks to the very high statistics and purity of the sources. Half-life values were extracted for the daughters ^{198g,m}At and ^{200}Fr, with similar or better precision compared with previous measurements. Several new fine-structure α-decay lines, with corresponding γ lines, were found in the decay chain of ^{202}Fr-^{198}At-^{194}Bi. Finally, the excitation energy of the isomer in ^{198}At could be determined at 265(3) keV due to the observation of a crossover transition in the fine-structure α decay of ^{202}Fr, which led to improved values for the excitation energy of the isomers in the α-decay chain ^{206}Ac-^{190}Tl.
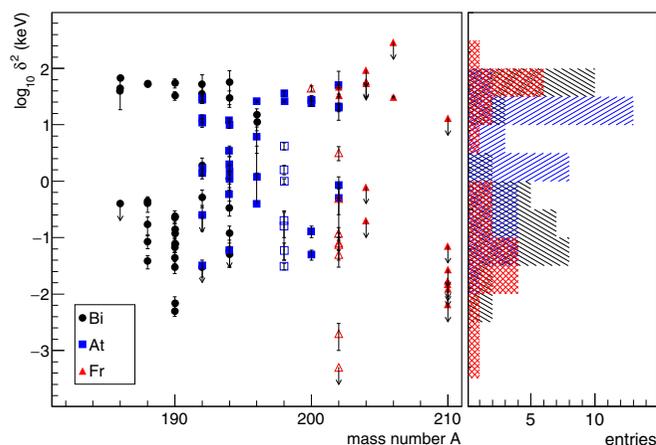
FIG. 11. Representation of the reduced widths for odd-odd At, Bi, and Fr nuclei in the region $N < 126$. Open symbols indicate the values deduced from this work, solid symbols represent literature values [4,5,11,28–30,32–34]. In most cases, each isomer has only one unhindered decay ($10 \lesssim \delta_\alpha^2 \lesssim 100$), while the other α-decay lines are hindered by at least a factor of 100.

[1] K. Heyde and J. L. Wood, Rev. Mod. Phys. **83**, 1467 (2011).

[2] B. A. Marsh, T. Day Goodacre, S. Sels, Y. Tsunoda, B. Andel, A. N. Andreyev, N. A. Althubiti, D. Atanasov, A. E. Barzakh, J. Billowes, K. Blaum, T. E. Cocolios, J. G. Cubiss, J. Dobaczewski, G. J. Farooq-Smith, D. V. Fedorov, V. N. Fedosseev, K. T. Flanagan, L. P. Gaffney, L. Ghys, M. Huyse, S. Kreim, D. Lunney, K. M. Lynch, V. Manea, Y. Martinez Palenzuela, P. L. Molkanov, T. Otsuka, A. Pastore, M. Rosenbusch, R. E. Rossel, S. Rothe, L. Schweikhard, M. D. Seliverstov, P. Spagnoletti, C. Van Beveren, P. Van Duppen, M. Veinhard, E. Verstraelen, A. Welker, K. Wendt, F. Wienholtz, R. N. Wolf, A. Zadvornaya, and K. Zuber, Nat. Phys. **14**, 1163 (2018).

[3] A. N. Andreyev, M. Huyse, and P. Van Duppen, Rev. Mod. Phys. **85**, 1541 (2013).

[4] P. Van Duppen, P. Decrock, P. Dendooven, M. Huyse, G. Reusen, and J. Wauters, Nucl. Phys. A **529**, 268 (1991).

[5] M. Huyse, P. Decrock, P. Dendooven, G. Reusen, P. Van Duppen, and J. Wauters, Phys. Rev. C **46**, 1209 (1992).

[6] C. Van Beveren, A. N. Andreyev, A. E. Barzakh, T. E. Cocolios, R. P. de Groote, D. Fedorov, V. N. Fedosseev, R. Ferrer, L. Ghys, M. Huyse, U. Köster, J. Lane, V. Liberati, K. M. Lynch, B. A. Marsh, P. L. Molkanov, T. J. Procter, E. Rapisarda, K. Sandhu, M. D. Seliverstov, P. Van Duppen, M. Venhart, and M. Veselský, J. Phys. G **43**, 025102 (2016).

[7] L. Ghys, A. N. Andreyev, M. Huyse, P. Van Duppen, S. Sels, B. Andel, S. Antalic, A. Barzakh, L. Capponi, T. E. Cocolios, X. Derkx, H. De Witte, J. Elseviers, D. V. Fedorov, V. N. Fedosseev, F. P. Hessberger, Z. Kalaninová, U. Köster, J. F. W. Lane, V. Liberati, K. M. Lynch, B. A. Marsh, S. Mitsuoka, P. Möller, Y. Nagame, K. Nishio, S. Ota, D. Pauwels, R. D. Page, L. Popescu, D. Radulov, M. M. Rajabali, J. Randrup, E. Rapisarda, S. Rothe, K. Sandhu, M. D. Seliverstov, A. M. Sjödin, V. L. Truesdale, C. Van Beveren, P. Van den Bergh, Y. Wakabayashi, and M. Warda, Phys. Rev. C **90**, 041301 (2014).

[8] K. Morita, Y. H. Pu, J. Feng, M. G. Hies, K. O. Lee, A. Yoshida, S. C. Jeong, S. Kubono, T. Nomura, Y. Tagaya, M. Wada, M. Kurokawa, T. Motobayashi, H. Ogawa, T. Uchibori, K. Sueki, T. Ishizuka, K. Uchiyama, Y. Fujita, H. Miyatake, T. Shimoda, T. Shinozuka, H. Kudo, Y. Nagai, and S. A. Shin, Z. Phys. A: Hadrons Nucl. **352**, 7 (1995).

[9] T. Enqvist, K. Eskola, A. Jokinen, M. Leino, W. H. Trzaska, J. Uusitalo, V. Ninov, and P. Armbruster, Z. Phys. A: Hadrons Nucl. **354**, 1 (1996).

[10] H. De Witte, A. N. Andreyev, S. Dean, S. Franchoo, M. Huyse, O. Ivanov, U. Köster, W. Kurcewicz, J. Kurpeta, A. Plochocki, K. Van de Vel, J. Van de Walle, and P. Van Duppen, Eur. Phys. J. A **23**, 243 (2005).

[11] Z. Kalaninová, S. Antalic, A. N. Andreyev, F. P. Hessberger, D. Ackermann, B. Andel, L. Bianco, S. Hofmann, M. Huyse, B. Kindler, B. Lommel, R. Mann, R. D. Page, P. J. Sapple, J. Thomson, P. Van Duppen, and M. Venhart, Phys. Rev. C **89**, 054312 (2014).

[12] G. T. Ewan, E. Hagberg, B. Jonson, S. Mattsson, and P. Tidemand-Petersson, Z. Phys. A: At. Nucl. **296**, 223 (1980).

[13] K. Eskola, P. Kuusiniemi, M. Leino, J. F. C. Cocks, T. Enqvist, S. Hurskanen, H. Kettunen, W. H. Trzaska, J. Uusitalo, R. G. Allatt, P. T. Greenlees, and R. D. Page, Phys. Rev. C **57**, 417 (1998).

[14] J. Uusitalo, M. Leino, T. Enqvist, K. Eskola, T. Grahn, P. T. Greenlees, P. Jones, R. Julin, S. Juutinen, A. Keenan, H. Kettunen, H. Koivisto, P. Kuusiniemi, A.-P. Leppänen, P. Nieminen, J. Pakarinen, P. Rahkila, and C. Scholey, Phys. Rev. C **71**, 024306 (2005).

[15] J. Stanja, C. Borgmann, J. Agramunt, A. Algora, D. Beck, K. Blaum, C. Böhm, M. Breitenfeldt, T. E. Cocolios, L. M. Fraile, F. Herfurth, A. Herlert, M. Kowalska, S. Kreim, D. Lunney, V. Manea, E. Minaya Ramirez, S. Naimi, D. Neidherr, M. Rosenbusch, L. Schweikhard, G. Simpson, F. Wienholtz, R. N. Wolf, and K. Zuber, Phys. Rev. C **88**, 54304 (2013).

[16] K. M. Lynch, J. Billowes, M. L. Bissell, I. Budinčević, T. E. Cocolios, R. P. De Groote, S. De Schepper, V. N. Fedosseev, K. T. Flanagan, S. Franchoo, R. F. Garcia Ruiz, H. Heylen, B. A. Marsh, G. Neyens, T. J. Procter, R. E. Rossel, S. Rothe, I. Strashnov, H. H. Stroke, and K. D. A. Wendt, Phys. Rev. X **4**, 011055 (2014).

[17] L. Ghys, Ph.D. thesis, KU Leuven, 2015.

[18] R. Harding (private communication).

[19] J. Wauters, P. Decrock, P. Dendooven, M. Huyse, P. Lievens, G. Reusen, and P. Van Duppen, Nucl. Instrum. Methods Phys. Res., Sect. B **61**, 178 (1991).

[20] B. Singh, Nucl. Data Sheets **107**, 1531 (2006).

[21] X. Huang and M. Kang, Nucl. Data Sheets **133**, 221 (2016).

[22] R. B. E. Taylor, S. J. Freeman, J. L. Durell, M. J. Leddy, S. D. Robinson, B. J. Varley, J. F. C. Cocks, K. Helariutta, P. Jones, R. Julin, S. Juutinen, H. Kankaanpää, A. Kanto, H. Kettunen, M. Leino, M. Muikku, P. Rahkila, A. Savelius, and P. T. Greenlees, Phys. Rev. C **59**, 673 (1999).

[23] T. Kibédi, T. Burrows, M. Trzhaskovskaya, P. Davidson, and C. Nestor, Nucl. Instrum. Methods Phys. Res., Sect. A **589**, 202 (2008).

[24] J. O. Rasmussen, Phys. Rev. **113**, 1593 (1959).

[25] H. Xiaolong, Nucl. Data Sheets **108**, 1093 (2007).

[26] C. M. Baglin, Nucl. Data Sheets **113**, 1871 (2012).

[27] M. Wang, G. Audi, A. H. Wapstra, F. G. Kondev, M. MacCormick, X. Xu, and B. Pfeiffer, Chin. Phys. C **36**, 1603 (2012).

[28] V. L. Truesdale, A. N. Andreyev, L. Ghys, M. Huyse, P. Van Duppen, S. Sels, B. Andel, S. Antalic, A. Barzakh, L. Capponi, T. E. Cocolios, X. Derkx, H. De Witte, J. Elseviers, D. V. Fedorov, V. N. Fedosseev, F. P. Heßberger, Z. Kalaninová, U. Köster, J. F. W. Lane, V. Liberati, K. M. Lynch, B. A. Marsh, S. Mitsuoka, Y. Nagame, K. Nishio, S. Ota, D. Pauwels, L. Popescu, D. Radulov, E. Rapisarda, S. Rothe, K. Sandhu, M. D. Seliverstov, A. M. Sjödin, C. Van Beveren, P. Van den Bergh, and Y. Wakabayashi, Phys. Rev. C **94**, 034308 (2016).

[29] A. N. Andreyev, D. Ackermann, F. P. Heßberger, S. Hofmann, M. Huyse, I. Kojouharov, B. Kindler, B. Lommel, G. Münzenberg, R. D. Page, K. V. de Vel, P. V. Duppen, and K. Heyde, Eur. Phys. J. A **18**, 55 (2003).

[30] A. N. Andreyev, S. Antalic, D. Ackermann, S. Franchoo, F. P. Heßberger, S. Hofmann, M. Huyse, I. Kojouharov, B. Kindler, P. Kuusiniemi, S. R. Lesher, B. Lommel, R. Mann, G. Münzenberg, K. Nishio, R. D. Page, J. J. Ressler, B. Streicher, S. Saro, B. Sulignano, P. Van Duppen, and D. R. Wiseman, Phys. Rev. C **73**, 024317 (2006).

[31] C. Qi, A. Andreyev, M. Huyse, R. Liotta, P. Van Duppen, and R. Wyss, Phys. Lett. B **734**, 203 (2014).

[32] A. N. Andreyev, D. Ackermann, S. Antalic, H. J. Boardman, P. Cagarda, J. Gerl, F. P. Heßberger, S. Hofmann, M. Huyse, D. Karlgren, A. Keenan, H. Kettunen, A. Kleinböhl, B. Kindler,

I. Kojouharov, A. Lavrentiev, C. D. O'Leary, M. Leino, B. Lommel, M. Matos, C. J. Moore, G. Münzenberg, R. D. Page, S. Reshitko, S. Saro, H. Schaffner, C. Schlegel, M. J. Taylor, K. V. de Vel, P. V. Duppen, L. Weissman, and K. Heyde, Eur. Phys. J. A **18**, 39 (2003).

[33] A. N. Andreyev, S. Antalic, D. Ackermann, L. Bianco, S. Franchoo, S. Heinz, F. P. Hessberger, S. Hofmann, M. Huyse,

I. Kojouharov, B. Kindler, B. Lommel, R. Mann, K. Nishio, R. D. Page, J. J. Ressler, P. Sapple, B. Streicher, S. Šáro, B. Sulignano, J. Thomson, P. Van Duppen, and M. Venhart, Phys. Rev. C **79**, 064320 (2009).

[34] P. Kuusiniemi, F. P. Heßberger, D. Ackermann, S. Hofmann, and I. Kojouharov, Eur. Phys. J. A **23**, 417 (2005).